Solar Heating Rates: The Importance of Spherical Geometry

D. J. LARY

Cambridge Centre for Atmospheric Science, Department of Chemistry, Cambridge University, Cambridge, United Kingdom

M. BALLUCH

Cambridge Centre for Atmospheric Science, Department of Applied Mathematics and Theoretical Physics, Cambridge University, Cambridge, United Kingdom

(Manuscript received 15 November 1992, in final form 23 March 1993)

ABSTRACT

A crucial component of any GCM is a scheme for calculating atmospheric heating rates. Since a detailed treatment of all processes involved is time consuming, many approximations are usually made. An approximation used in virtually all GCM radiation codes that extend into the middle atmosphere is that the atmosphere can be treated as plane parallel. This approximation breaks down when the sun is close to the horizon and does not apply for large solar zenith angles. This paper shows that this approximation leads to a very serious underestimate of solar heating rates in the polar regions. Ignoring spherical effects, and in particular the heating due to absorption at zenith angles greater than 90°, gives rise to a very different latitudinal gradient in the diurnally averaged heating rates calculated at the equinox. Such a change in the latitudinal gradient in the heating rate is of significance for the general circulation. Accounting for the heating that occurs at zenith angles greater than 90° is shown to be important.

1. Introduction

Radiation incident on the atmosphere embodies the ultimate driving force for all the atmospheric processes that occur. One of the major difficulties in computing the solar radiation field in a spherical atmosphere is an accurate description of multiple scattering. The motivation of this study is to assess the importance of spherical geometry for solar heating at zenith angles greater than 90° (the hashed region shown in Fig. 1) in a model that contains a detailed description of all orders of multiple scattering. This is part of a larger study that aims to develop schemes to calculate heating and photolysis rates in a consistent, accurate, and computationally efficient manner. These schemes are intended for use in general circulation models that also contain a detailed description of atmospheric chemistry.

2. Model description

The model solves the static radiation transport equation with spherical symmetry:

$$\mu \frac{\partial I}{\partial r} + \frac{1-\mu^2}{r} \frac{\partial I}{\partial \mu} = \sigma_e (S - I). \quad (1)$$

Here I is the specific intensity, r is the distance to the center of the earth, μ is the cosine of the angle to the outward normal, S is the source function, and σ_e is the extinction coefficient, which has two components, the true absorption coefficient and the scattering coefficient, $\sigma_e = \sigma_a + \sigma_s$. A reflectional symmetry is used for the azimuthal variation in the radiation field about the vertical plane spanned by the incoming light rays from the sun and the column of atmospheric air under consideration. In order to calculate the radiation field for a given column, we neglect the variation of the physical state of the surrounding atmosphere with latitude and longitude.

With these assumptions, the characteristics of Eq. (1), which is a parabolic differential equation, can be found analytically. These characteristics are the curves p = const, where p is defined as

$$p = r\sqrt{1-\mu^2}. \quad (2)$$

If we introduce these characteristics as new coordinates, we end up with an ordinary differential equation that looks very similar to the plane parallel case:

$$\frac{dI}{d(\mu r)} = \sigma_e (S - I). \quad (3)$$

With the help of the Laplace transformation, this equation can be solved analytically, leading to

$$I(\tau) = e^{-\tau} I(\tau = 0) + e^{-\tau} \int_0^\tau e^x S(x) dx, \quad (4)$$

Corresponding author address: Dr. David J. Lary, Department of Chemistry, University of Cambridge, Lensfield Road, Cambridge, UK, CB2 1EW.

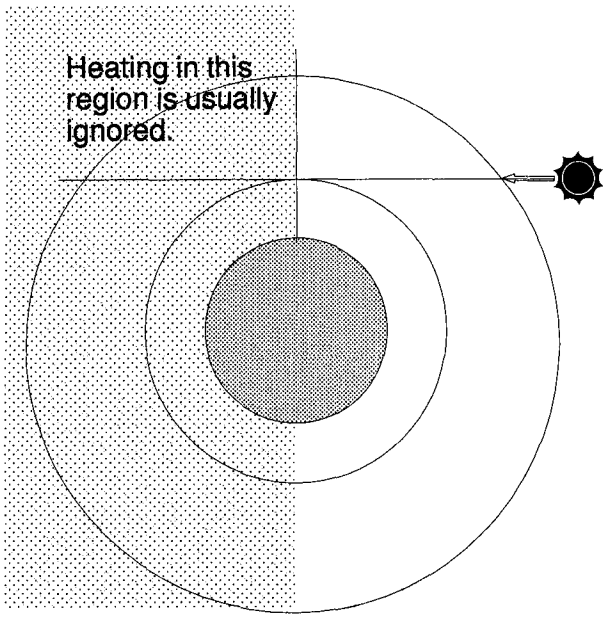

FIG. 1. When the plane parallel approximation is made in calculating atmospheric heating rates, the hashed region is completely ignored.

where the optical depth τ is defined differentially as

$$d\tau = \sigma_e d(\mu r). \tag{5}$$

In this way Eq. (1) can be solved by numerically integrating the second term on the right-hand side of Eq. (4) as well as Eq. (5) for each characteristic. The source function is thereby generally approximated using the LTE assumption by

$$S(r, \mu) = \frac{\sigma_a(r)B(r) + \sigma_s(r)\frac{1}{2}\int_{-1}^{1} I(r, \hat{\mu})\rho(\mu'(\mu, \hat{\mu}))d\hat{\mu}}{\sigma_e(r)}; \tag{6}$$

where B denotes the Planck function for thermal emission, which can safely be neglected for the frequencies we are concerned with here, and ρ denotes the phase function, which is a normalized distribution function for scattered light. In the calculations presented here, isotropic scattering was assumed and therefore ρ was set to unity. In this case the source function is independent of μ and the azimuth.

The general procedure for solving this problem is as follows. First we calculate the direct beam, assuming $S = 0$, for all zenith angles. For each height level (we used 96 in all the calculations presented), we choose a specific characteristic, that is, a specific curve p = const, that meets a sphere of constant radius exactly at the zenith angle under consideration. So, for each height level we have a different, uniquely defined characteristic, since each value of p leads to exactly one incoming angle from the side of the sun for a given height. With the use of Eq. (6) we can calculate the contribution to S coming from the direct beam. Now we choose a different set of characteristics (120 in our calculations) that covers the whole range of angles for each height level well enough to allow a sufficiently accurate Simpson integration over μ as in Eq. (6). Each characteristic corresponds to four lines of sight since a given value of the modulus of the cosine of an angle corresponds to four different angles. We now integrate Eq. (4) along all characteristics separately and perform the μ integration of Eq. (6) to get a modified source function, which could be used to solve (4) again along all characteristics leading to a new source function and so on. An accurate solution of Eq. (1) will provide us, via integration over μ, with the enhancement factor and eventually with the heating rates as well.

The iterative solution was considered to be sufficiently accurate when the Eddington, or anisotropy, factor changed by less than 10^{-5}. The iteration procedure converged surprisingly fast, needing between 3 and 20 iterations for each of the 203 frequency bands and 42 zenith angles considered. For details of this method, other applications, and a more general formulation see Balluch (1986) or Balluch (1988).

3. Results

The purpose of this section is to investigate the roles of spherical geometry and multiple scattering in the calculation of atmospheric heating rates, and to compare the relative computational costs involved. This is of particular relevance since many radiative transfer models in current usage make the plane parallel approximation and do not contain a detailed treatment of multiple scattering.

Before considering in detail the effects of spherical geometry, it is instructive to consider how much the various spectral regions contribute to the total solar heating rate. Based on the features of the ozone absorption cross section (see Fig. 2), the spectral region that was considered in this study (121 nm to 850 nm) was divided up into four parts.

Name	λ (nm)	Comments
(a)	121–201	Makes only a small contribution
(b)	201–255	The peak O_3 absorption occurs at 255 nm
(c)	255–360	Transition from strongly absorbing to weakly absorbing atmosphere
(d)	360–850	Little absorption occurs

Of these spectral regions, part (c) is the most important, making a large contribution to the solar heating rate at all altitudes. In the upper stratosphere and lower mesosphere, part (b) is also important, although not dominant. Part (d), the visible region, makes its largest contribution in the lower stratosphere, partic-

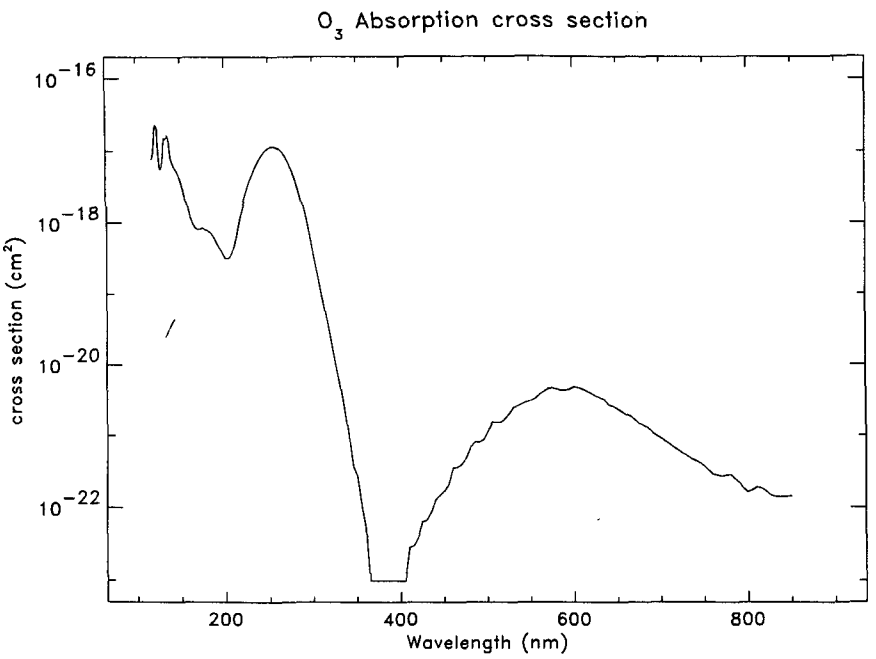

FIG. 2. The O_3 absorption cross section used in this study.

ularly below 30 km, and starts to dominate below about 26 km.

It is interesting to note that the altitude at which the heating rate maximum occurs changes with the solar zenith angle (as can be seen in Fig. 4). This is because of the shape of the ozone profile. The ozone profile used in this study is a typical midlatitude summer ozone profile and is shown in Fig. 3. The ozone volume mixing ratio (vmr) peaks at around 30 km. Between 50 km and 65 km there is another smaller "feature" where the vmr remains greater than 0.5 ppmv. When the sun is overhead, and hence, the direct beam traverses a relatively short path through the atmosphere, most of the solar energy is deposited due to the large absorption that occurs quite low down in the atmosphere at an altitude corresponding to the highest ozone concentrations (close to 30 km). However, because the density of the atmosphere decreases exponentially with increasing altitude, the largest heating rates are seen not at this altitude, but in the upper stratosphere, close to 45 km (see, for example, Fig. 4a). As the sun gets closer to the horizon, the total pathlength through the atmosphere traversed by direct sunlight increases. This leads to more absorption of sunlight, and hence deposition of energy, at higher altitudes due to the "feature" in the ozone vmr profile between approximately 50 km and 65 km. Consequently, less sunlight reaches the region of larger ozone concentrations, and so less energy is deposited lower down in the atmosphere, and the altitude of the heating rate maximum increases (see, for example, Fig. 4a). It can be seen very clearly from Fig. 4a that in the upper stratosphere and lower mesosphere *substantial* heating can still occur for zenith angles *greater* than 90°, that is, even when the sun has set at the surface of the earth and the plane parallel atmosphere becomes undefined.

a. Effects of spherical geometry on the heating rate calculations

This section quantifies the effect of assuming that the atmosphere is plane parallel, for both the treatment of the direct beam and the multiply scattered light, when calculating atmospheric heating rates. Figure 4a shows the instantaneous atmospheric heating rate in kelvin per day for a ground albedo of

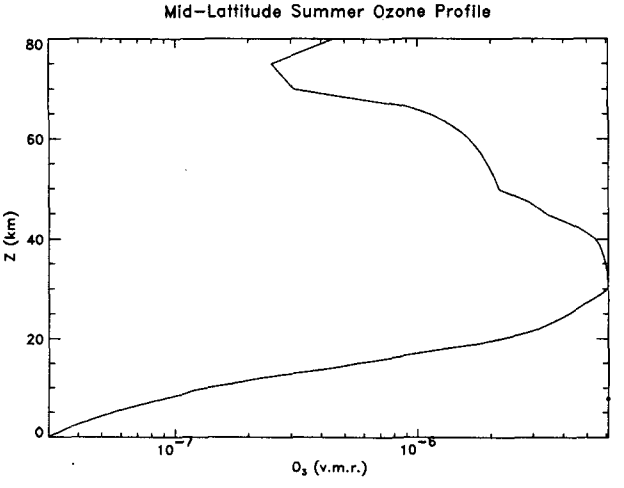

FIG. 3. The midlatitude summer O_3 profile used in this study.

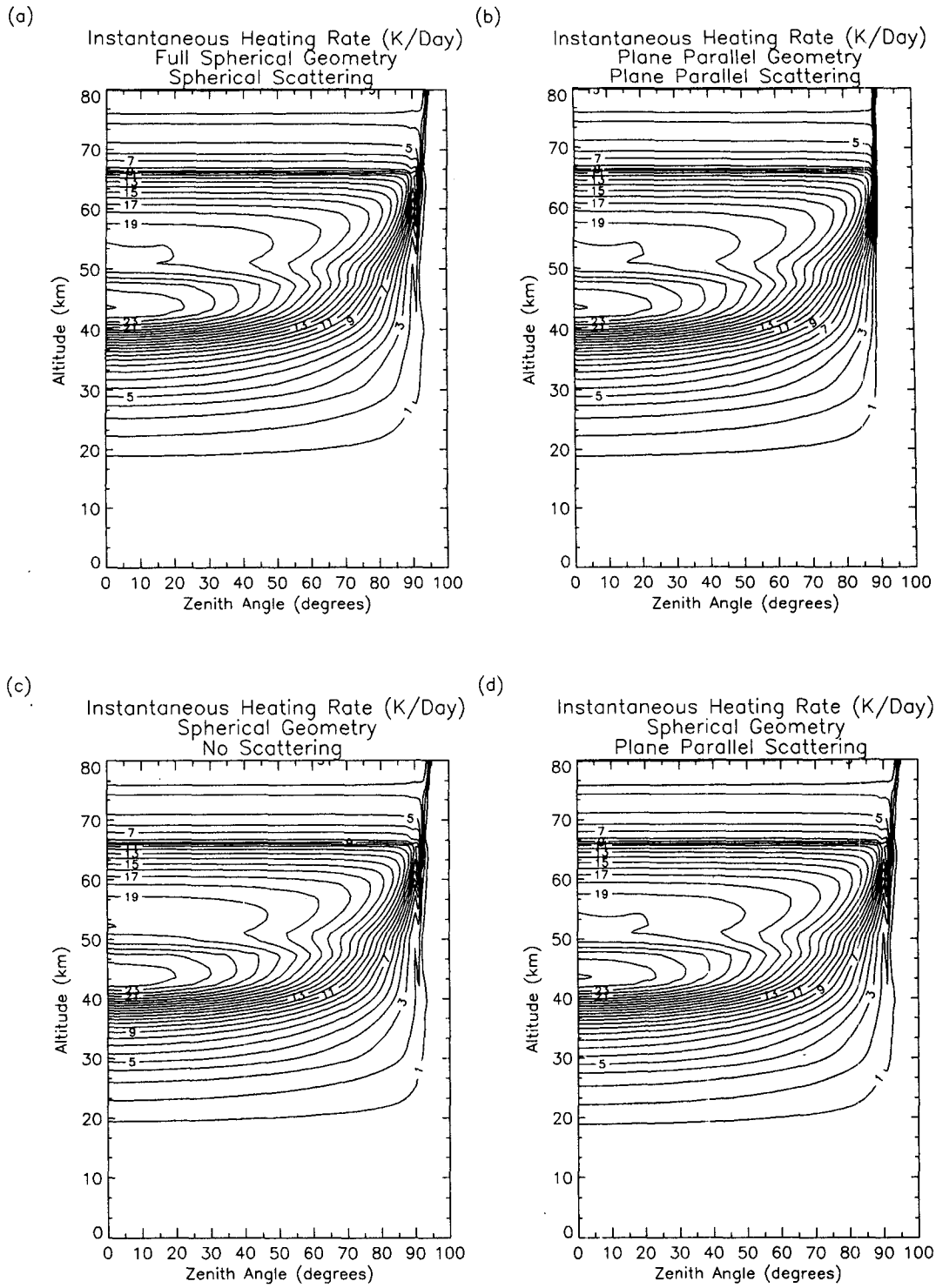

FIG. 4. The instantaneous heating rate as a function of zenith angle and altitude calculated in four different ways. (a) Full spherical geometry with spherical multiple scattering, (b) plane parallel geometry with plane parallel multiple scattering, (c) full spherical geometry with no multiple scattering, (d) spherical geometry direct beam with plane parallel multiple scattering. The contour interval is 1 K day^{-1}, with contours starting at 1 K day^{-1}.

0.5 as a function of zenith angle in degrees on the x axis and altitude in kilometers on the y axis. The calculation included a full treatment of spherical geometry for both the direct beam and the multiply scattered light. Figure 4b is the analogous calculation made for a plane parallel atmosphere. A salient feature of Fig. 4b is the region of *no heating* for zenith angles greater than 90° since these zenith angles are undefined in a plane parallel atmosphere. Figure 5a shows the absolute difference between these two calculations. It can be seen from Fig. 5a that the plane parallel approximation leads to a small overestimate of the heating rate above 10 km for zenith angles less than 55° throughout the stratosphere. The largest overestimate is just over 0.03 K day^{-1} and occurs for an overhead sun. The breakdown of the plane parallel approximation starts to occur at a zenith angle of 55° at just above 40 km. This is noteworthy since it is normally assumed that the plane parallel approximation starts to breakdown at a zenith angle of 75°. The largest underestimate of the heating rate due to using the plane parallel approximation occurs in the region close to 65 km for a zenith angle of around 91°, where it reaches more than 9 K day^{-1} (the contours in Fig. 5 are on a logarithmic scale). However, an underestimate of greater than 1 K day^{-1} covers a much larger region, extending down to lower than 30 km. The role that multiple scattering plays will be considered in the next subsection.

The results of taking the heating rate calculations shown in Figs. 4a and 4b and using them to calculate diurnal average heating rates for the solstice and the equinox are shown in Fig. 7. The differences between the two can be found in Fig. 8 as both absolute and percentage differences.

At the equinox the underestimate of the heating rate that results from making the plane parallel approximation is important since all the heating that is occurring at zenith angles greater than 90° is completely ignored. This has a marked effect on the latitudinal structure of the diurnal average heating rate. This can be seen by comparing Fig. 7a and Fig. 7b. Figure 7a shows the diurnal average heating rate calculated for the equinox assuming a full spherical geometry, whereas Fig. 7b shows the analogous calculation made using the plane parallel approximation. Using the plane parallel approximation at the equinox causes two types of inaccuracy. The first inaccuracy is a complete change in the *shape* of the latitudinal heating rate gradient at the equinox. In the spherical case (Fig. 7a), all the contours up to and including the 6 K day^{-1} contour are open and extend right to the poles, with a relatively shallow latitudinal gradient in the solar heating rate at middle and low latitudes, with the 1 K day^{-1} contour at close to 30 km virtually horizontal. On the other hand, in Fig. 7b, which shows the plane parallel calculation, the contours are all closed and never reach the poles. Figure 8c shows that close to the two poles, using the plane parallel approximation leads to an underestimate of the heating rate of more than 40%. The second inaccuracy is an underestimate of the polar heating rate of up to 7 K day^{-1} at the poles at an altitude of around 65 km. A noticeable underestimate of the heating rate extends over a much wider region.

The change in the calculated latitudinal heating rate gradient that occurs when spherical geometry is included will affect the temperature gradients calculated by a numerical model, particularly in polar regions, and may also affect the general circulation calculated by the model. Although the magnitude of this change in the general circulation has not been quantified in this paper, it is likely to be significant, because an examination of Fig. 8d shows that at the winter solstice the heating rate poleward of approximately 60° is underestimated by at least 20% if the heating rate is calculated using plane parallel geometry. Ramanathan et al. (1983) found that in a general circulation model the impact of a change in the temperature gradient between equator and pole due to changes in the radiative heating was significant. This was the case even though the changes were smaller than those suggested by Figs. 8c and 8d.

The error due to making the plane parallel approximation is generally smaller at the solstice than the equinox. Nonetheless, there are some differences that are most evident at the polar day and polar night boundaries. For both of these situations the earth's atmosphere is illuminated for long periods by radiation incident at high solar zenith angles. In this region an underestimate of the heating rate of up to 1 K day^{-1} can occur at 65 km. In percentage terms, the largest error due to making the plane parallel approximation occurs at the winter pole where the heating rate, although small in absolute terms, is underestimated by *more than 90%* for all latitudes poleward of the polar circle. At the polar day boundary the error can exceed 5% between 10 km and 35 km, and be greater than 10% above 65 km.

b. *Effects of multiple light scattering on the heating rate calculations*

To investigate the effects of multiple scattering on the calculation of heating rates the results of three different model runs were compared, each using spherical geometry for the direct beam but different treatments of multiple scattering: namely, scattering in spherical geometry, scattering in plane geometry, and no scattering at all. The differences between these calculations are largest, as might be expected, at around 40 km, where the heating rate reaches its maximum value (Fig. 5).

An examination of Fig. 5d shows that for all zenith angles ignoring multiple scattering leads to an *underestimate* of the heating rate. In absolute terms the underestimate is largest for a zenith angle of 0°, where it peaks at around 0.6 K day^{-1} at approximately 35 km.

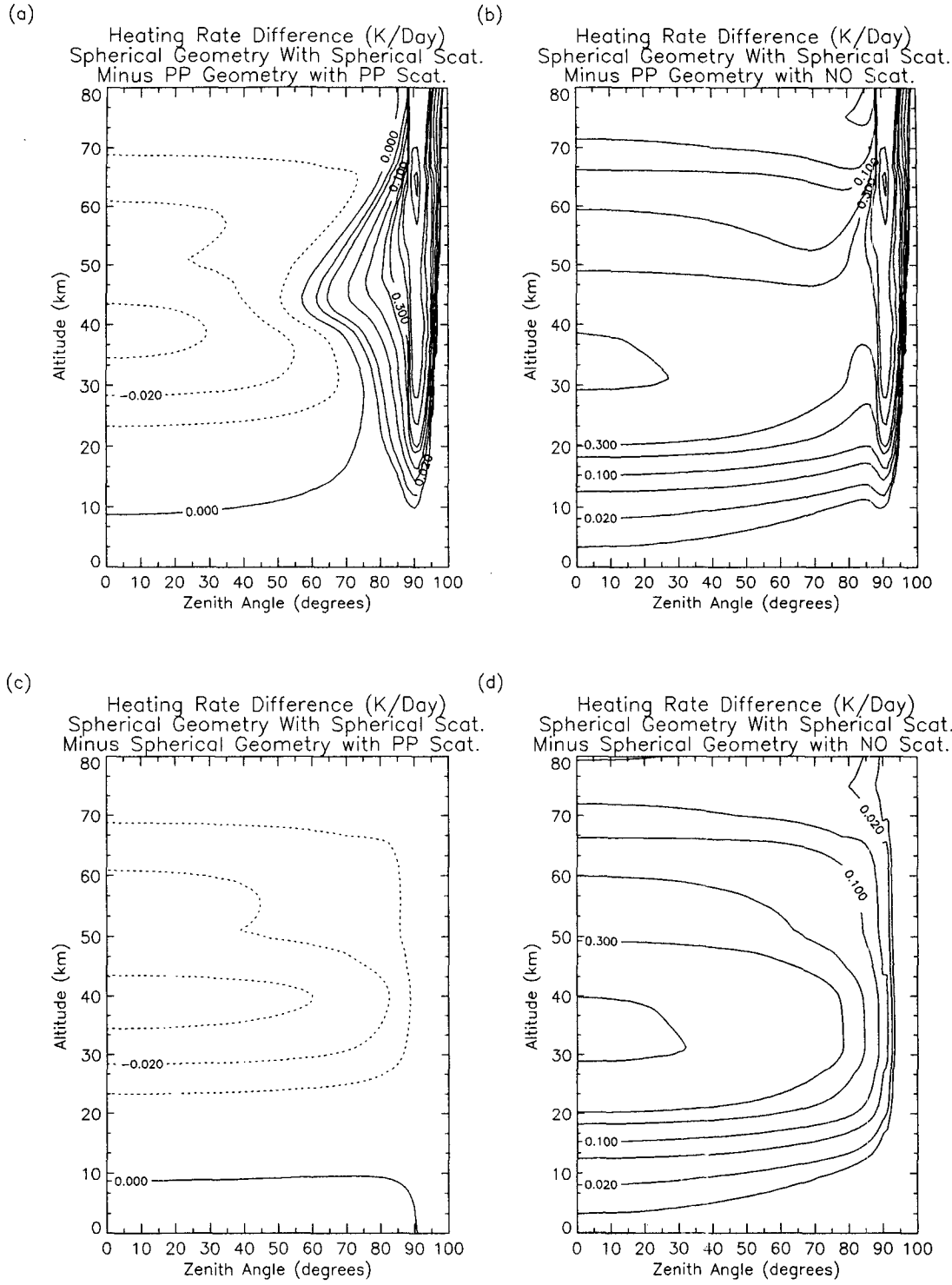

FIG. 5. The absolute difference in the instantaneous heating rate calculations as a function of zenith angle and altitude. Note that the contour interval is logarithmic.

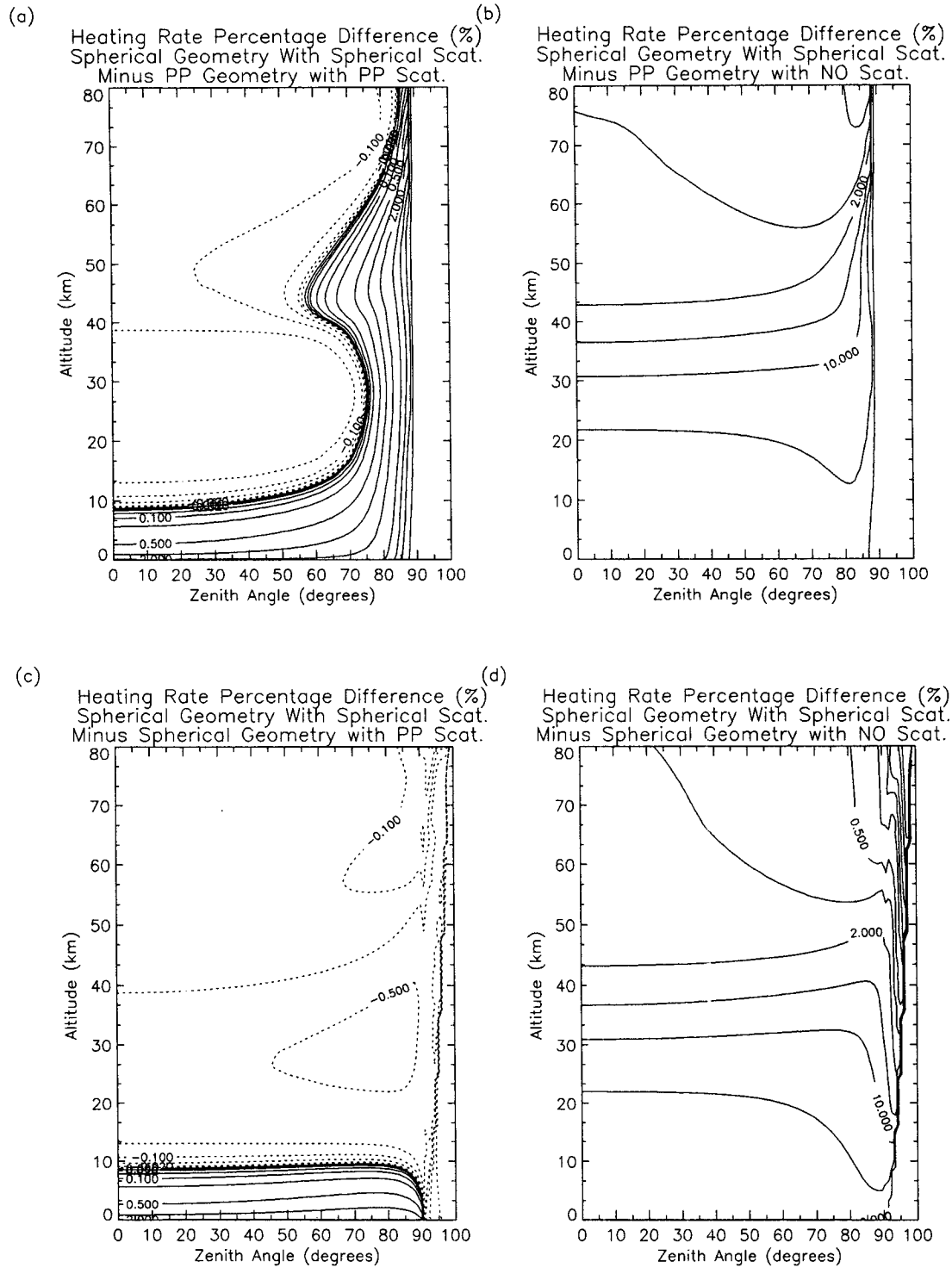

The contour levels are: [−10,−5,−2,−1,−0.5,−0.2,−0.1,−0.05,−0.02,−0.01,0,0.01,0.02,0.05,0.1,0.2,0.5,1.,2.,5.,10.,20.,50.]
Dashed contours are less than zero.

FIG. 6. The percentage difference in the instantaneous heating rate calculations as a function of zenith angle and altitude. Note that the contour interval is logarithmic.

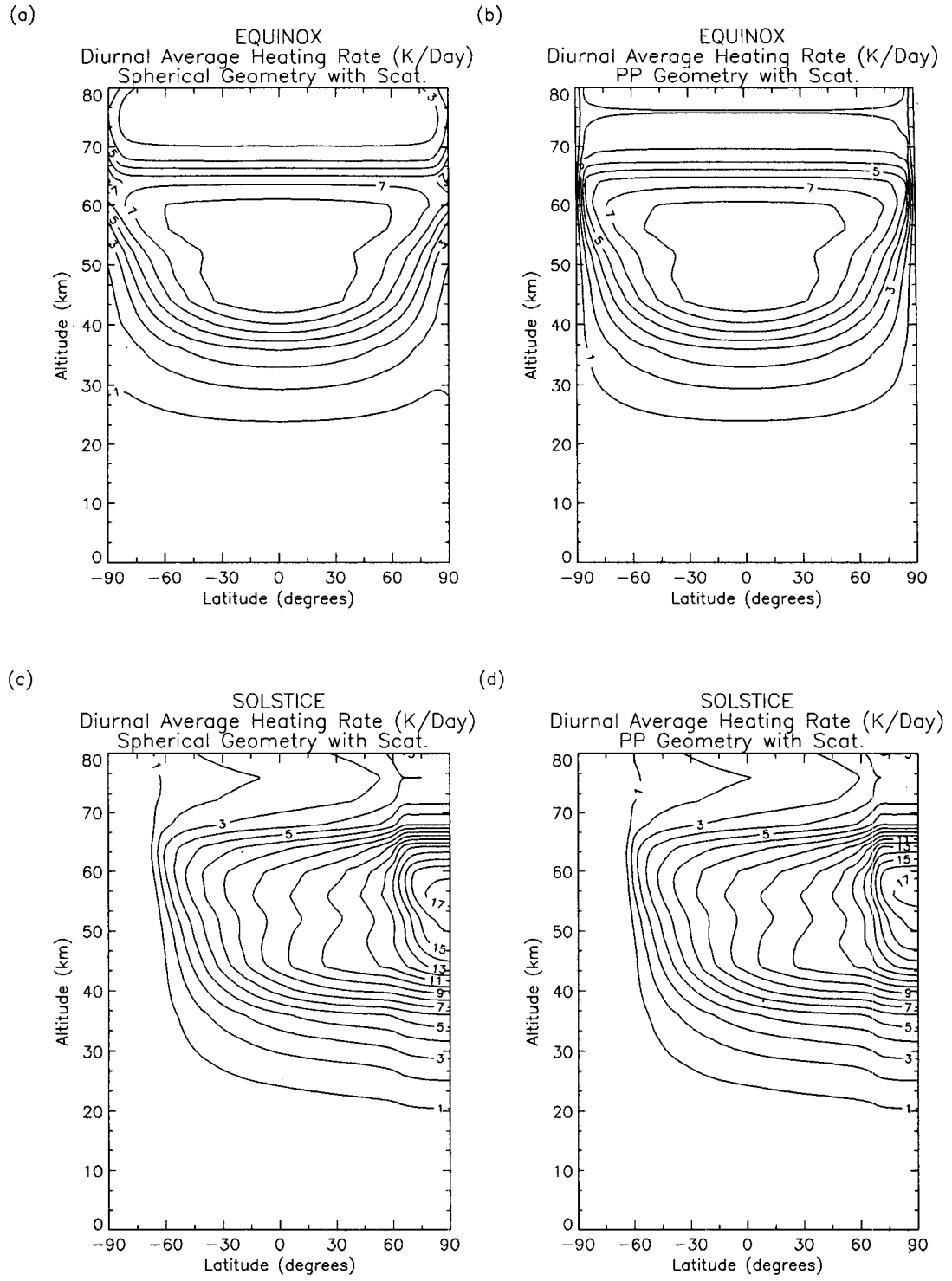

FIG. 7. The diurnal average heating rate for the solstice and equinox as calculated using a full spherical geometry with spherical multiple scattering (a and c) and using a plane parallel geometry with plane parallel multiple scattering (b and d). The contour interval is 1 K day^{-1}, and contours start at 1 K day^{-1}.

However, in percentage terms, the error is greater than 20% below 20 km where the number of scatterers is largest and the heating rate is relatively small (Fig. 6d). In absolute terms the underestimate decreases as the zenith angle increases, whereas in percentage terms the underestimate increases rapidly at zenith angles greater

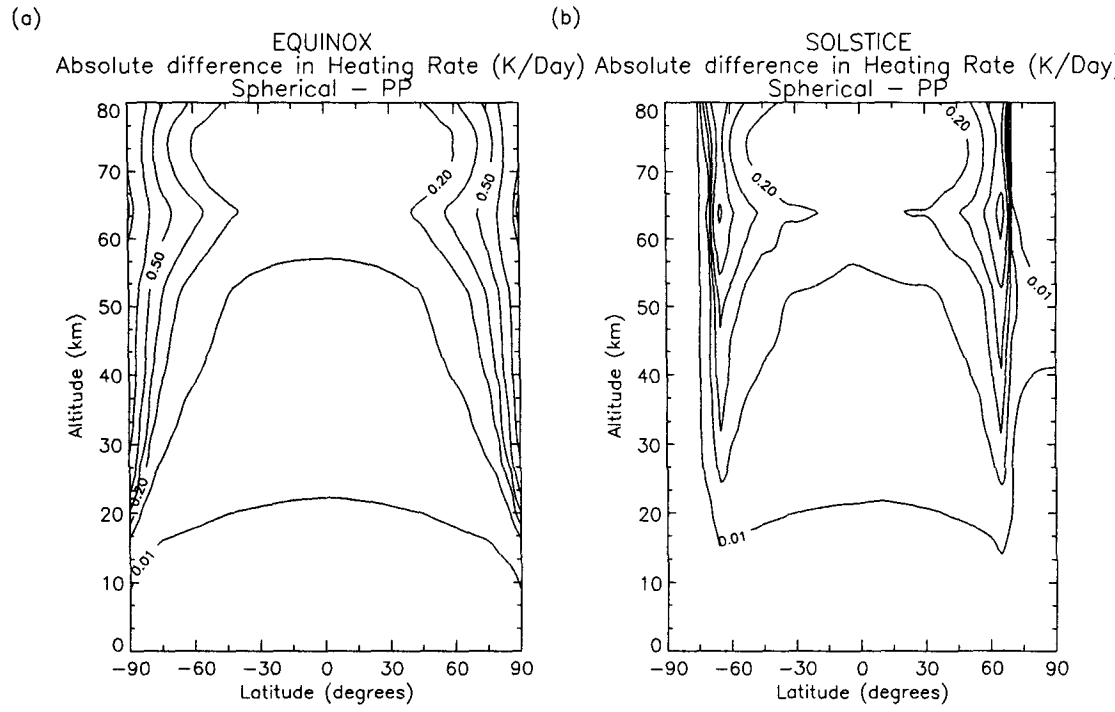

FIG. 8. The difference in the diurnal average heating rate (in absolute and percentage terms) for the solstice and equinox calculated using a full spherical geometry with spherical multiple scattering and using a plane parallel geometry with plane parallel multiple scattering.

than 90°. This is because for long atmospheric pathlengths, multiple scattering will divert light from the direct solar beam, thus lowering the heating that occurs due to the absorption of the direct beam alone. However, the light scattered out of the direct beam should not be ignored as it can also be absorbed and lead to atmospheric heating. Ignoring multiple scattering does not allow this process to occur in the model. Therefore, including a description of multiple scattering is more important when spherical geometry is used. (Please note that when ignoring multiple scattering is mentioned in the text, the extinction of the direct beam by light scattering out of the direct beam is included. Inclusion of this extinction of the direct beam by scattering is important.)

Looking at the differences between the full spherical scattering calculation and the calculation where scattering is performed in a plane parallel geometry (Fig. 5c), we find that the differences are far smaller than those of the "no scattering" case (Fig. 5d). Indeed, the absolute maximum reaches about 0.04 K day^{-1} at a height of around 40 km in the case of small zenith angles. In conclusion, the plane parallel scattering model provides us with results having an error of less than 1% (Fig. 6c), which is two orders of magnitude larger than the overall discretization error. We determined the latter by increasing the resolution in the discretization of the angles to up to 2000 angles for 360 degrees, finding that the errors rapidly decrease. The finest resolution compared to the runs described here had a relative difference of 0.01% in the maximum. In contrast to the case of no scattering at all (Fig. 5d), the case of plane parallel scattering represents well the heating rate in the troposphere and at high zenith angles.

c. *Effects of the ground albedo on the heating rate calculations*

In all the calculations presented so far, a ground albedo of 0.5 has been used. Therefore, we may ask whether changing the ground albedo would significantly affect the results already presented.

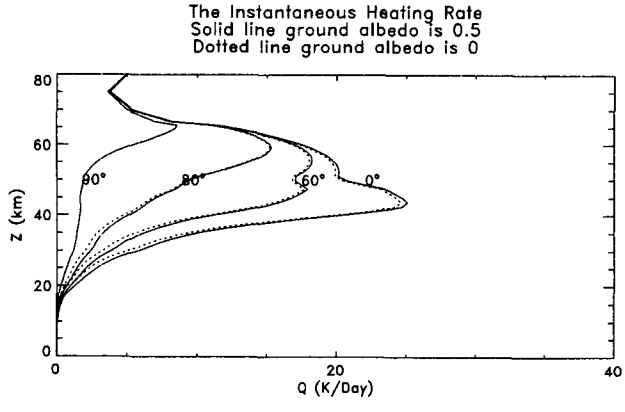

FIG. 9. The effect of different ground albedos on the instantaneous heating rate for a range of zenith angles.

TABLE 1. The computational costs for solar zenith angles of 0° and 85°.

Type of calculation	Normalized CPU time
(a) Solar zenith angle of 0°	
Spherical direct beam with spherical scattering	9179
Spherical direct beam with plane parallel scattering	9100
Plane parallel direct beam with plane parallel scattering	8851
Spherical direct beam	129
Plane parallel direct beam	1
(b) Solar zenith angle of 85°	
Spherical direct beam with spherical scattering	7881
Spherical direct beam with plane parallel scattering	7415
Plane parallel direct beam with plane parallel scattering	7321
Spherical direct beam	108
Plane parallel direct beam	1

Figure 9 shows a comparison of heating rates for ground albedos of 0 and 0.5 calculated at different zenith angles. For a zenith angle of 0° (an overhead sun) the difference is largest, whereas for a zenith angle 90° (the sun at the horizon) the difference is zero. The altitude range where the differences are largest in absolute, as well as in relative, terms is between 20 km and 30 km.

In the regions where the difference is largest between the spherical and plane parallel calculations, the ground albedo plays little or no role. This is because at large zenith angles much less light reaches the surface of the earth, and at zenith angles greater than 90° no direct sunlight reaches the surface. Consequently, a change in the heating rate due to a change in the ground albedo is quite small, especially in the upper stratosphere and mesosphere. However, by changing the ground albedo from 0 to 0.5, the small error that occurs when the multiply scattered component is calculated in a plane parallel atmosphere is increased by a factor of up to 3 when compared to the spherical calculation. If scattering is completely ignored, then the error can increase by a factor of $3\frac{1}{2}$.

d. *The computational costs*

When considering the practical implications of our results for numerical models, it is interesting to investigate the computational cost involved in the various treatments of multiple scattering and spherical geometry. Table 1 shows the CPU execution times on a CRAY X/MP for our model with 96 vertical layers, 120 characteristics, and 203 wavelength intervals. In each case the times are normalized to the fastest run, which was the plane parallel direct beam calculation. Table 1a shows the results for a solar zenith angle of

0° (where the plane parallel direct beam calculation took 9.86×10^{-3} s), and Table 1b the corresponding situation for a solar zenith angle of 85° (the plane parallel direct beam calculation took 1.03×10^{-2} s).

Let us consider first the computer time required for just the direct solar radiation. When the atmosphere is treated as a set of plane parallel slabs, a given light ray from the sun meets all the layers of the atmosphere at the *same* zenith angle. However, in reality, there is a spherical geometry and at each altitude a given light ray will intersect the atmosphere at *different* solar zenith angles. Therefore, the calculation time required for a full spherical geometry is approximately the number of model layers multiplied by the time required for the plane parallel calculation. When multiple scattering is included, many different light rays have to be considered, not just the direct light ray coming from the sun; consequently, even for the plane parallel atmosphere, including multiple scattering causes a large increment in the computer time required.

The calculation for a solar zenith angle of 85° took about five-sixths of the time required for the overhead sun calculation in all three cases. If the effects of scattering are included, then it seems that there is not much CPU time saved by using anything less than the full spherical calculation. Although it should be stated that the differences between the full spherical calculation, and the calculation where the direct beam is treated using spherical geometry and scattering calculated using plane parallel geometry differ in the resulting heating rate by less than 1%. The latter uses less CPU time than the full spherical calculation.

To get an idea of what the minimum CPU time required for a full spherical treatment with reasonable error would be, the characteristics and the cutoff parameter for the iteration procedure were reduced until the results differed by more than one percent in the heating rate. It turned out that the model is quite robust and the minimum number of characteristics was 8 (corresponding to a 32 angle discretization for a 360° circle) and the minimum cutoff parameter was 10^{-2}. With these parameters the full spherical calculation for an overhead sun took 199 of the normalized CPU time units used in Fig. 10a and for a solar zenith angle of 85°, 176 normalized CPU time units used in Fig. 10b. Since the calculation of the direct beam has not been altered, most of the CPU time is now spent on the direct beam calculation, and the time required to calculate the scattered component has been reduced by a factor of more than 100.

4. Summary

Using the plane parallel approximation leads to a significant underestimate of the solar heating rate, especially in polar regions. A model that uses the plane parallel approximation cannot account for the significant heating that occurs due to the absorption of solar radiation at solar zenith angles greater than 90°. This in turn leads to an unrealistically large latitudinal heating rate gradient at the equinoxes. When the plane parallel approximation is used for equinox conditions, the atmospheric heating rate is underestimated by more than 40% at all altitudes at the poles. At the winter solstice heating close to, and within, the polar circle is underestimated by more than 90%. Close to the heating rate maximum, the plane parallel approximation begins to break down at solar zenith angles less than 75°.

Since the vertical velocity is dependent on the local heating rate, models that use a plane parallel geometry to calculate solar heating rates will misrepresent the structure of the general circulation, particularly in the region close to the polar night (and polar day) boundary. The exact magnitude of this effect is beyond the scope of this study.

The importance of including multiple scattering from air molecules is less than the importance of spherical geometry, but is most significant for very large solar zenith angles and below an altitude of 20 km. Describing scattering in a plane parallel geometry, while calculating the direct beam in spherical geometry, shows very good agreement with the full spherical calculation, particularly for large zenith angles, where the scattering plays its biggest role. However, comparison of the CPU times using our particular model shows that there is not much time to be saved by calculating scattering in this way.

Acknowledgments. The authors would like to thank J. Kiehl, K. Shine, and M. McIntyre for useful conversations. This work received support from the Natural Environment Research Council through the UK Universities' Global Atmospheric Modelling Project, and through Grant GR9/515A, from the Innovative Science and Technology Program through Grant N00014-92-J-2009 administered by the US Naval Research Laboratory, and from the DGXII of the CEC and the STEP programme of the CEC.

REFERENCES

Anderson, D. E., 1983: The troposphere to stratosphere radiation field at twilight: A spherical model. *Planet. Space Sci.*, **31**, 1517–1523.

Balluch, M., 1986: Numerische Lösung einer Differentialgleichung 1. Ordnung mit der Methode der Charakteristiken am Beispiel der Stahlungstransportgleichung. M. S. thesis, University of Vienna.

——, 1988: *Astron. Astrophys.*, **200**, 58–74.

Morcrette, J. J., 1990: Impact of changes to the radiation transfer parameterizations plus cloud optical properties in the ECMWF model. *Mon. Wea. Rev.*, **118**, 847.

Ramanathan, V., E. J. Pitcher, R. C. Malone, and M. L. Blackmon, 1983: The response of a spectral general circulation model to refinements in radiative processes. *J. Atmos. Sci.*, **40**, 605.